Quantification of topographic venting of boundary layer air to the free troposphere

S. Henne, M. Furger, S. Nyeki, M. Steinbacher, B. Neininger, S. F. J. de Wekker, J. Dommen, N. Spichtinger, A. Stohl, André S. H. Prévôt

Atmos. Chem. Phys. Discuss., 3, 5205–5236, 2003
www.atmos-chem-phys.org/acpd/3/5205/

Atmospheric Chemistry and Physics Discussions

Quantification of topographic venting of boundary layer air to the free troposphere

S. Henne[1], M. Furger[1], S. Nyeki[1, 2], M. Steinbacher[1], B. Neininger[3], S. F. J. de Wekker[1, *], J. Dommen[1], N. Spichtinger[4], A. Stohl[4, †], and A. S. H. Prévôt[1]

[1]Paul Scherrer Institut, Villigen, Switzerland
[2]University of Essex, Colchester Essex, UK
[3]MetAir AG, Illnau, Switzerland
[4]Lehrstuhl für Bioklimatologie und Immissionsforschung, Technical University of Munich, Freising, Germany
[*]Current affiliation: Pacific Northwest National Laboratory, Richland, Washington, USA
[†]Current affiliation: NOAA Aeronomy Laboratory, Boulder, Colorado, USA

Received: 21 August 2003 – Accepted: 25 September 2003 – Published: 16 October 2003

Correspondence to: A. S. H. Prévôt (andre.prevot@psi.ch)

Abstract

Net vertical air mass export by thermally driven flows from the atmospheric boundary layer (ABL) to the free troposphere (FT) above deep Alpine valleys was investigated. The vertical export of pollutants above mountainous terrain is presently poorly represented in global chemistry transport models (GCTMs) and needs to be quantified. Air mass budgets were calculated using aircraft observations obtained in deep Alpine valleys. The results show that on average 3 times the valley air mass is exported vertically per day under fair weather conditions. During daytime the type of valleys investigated in this study can act as an efficient "air pump" that transports pollutants upward. The slope wind system within the valley plays an important role in redistributing pollutants. Nitrogen oxide emissions in mountainous regions are efficiently injected into the FT. This enhances their ozone production efficiency and thus influences tropospheric pollution budgets. Once lifted to the FT above the Alps pollutants are transported horizontally by the synoptic flow and are subject to European pollution export. Forward trajectory studies show that under fair weather conditions two major pathways for air masses above the Alps dominate. Air masses moving north are mixed throughout the whole tropospheric column and further transported eastward towards Asia. Air masses moving south descend within the subtropical high pressure system above the Mediterranean.

1. Introduction

Nitrogen oxides ($NO_x = NO_2 + NO$) and volatile organic compounds (VOC) govern ozone production in the troposphere (Seinfeld and Pandis, 1998). Most anthropogenic and biogenic emissions of NO_x and VOCs take place in the ABL. The ozone production efficiency, which is the number of O_3 molecules produced by each NO_x molecule consumed (Lin et al., 1988), is enhanced by transport to the FT (Seinfeld and Pandis, 1998). Once the air mass has left the ABL, dry deposition of NO_x and O_3 ceases and leads to an increased lifetime of these species. As temperatures decrease in the tro-

ACPD

3, 5205–5236, 2003

posphere with increasing altitude the reaction of NO with O_3 is decelerated. Therefore the photostationary state of the O_3 – NO_x cycle is shifted to a higher NO/NO_2 ratio. In addition peroxyacetyl nitrate (PAN) can act as a reservoir species for NO_2 at lower temperatures. The lower the concentration of NO_2 the more OH radicals react with hydrocarbons and therefore enhance ozone production (as long as NO > 10 – 30 pptv). Mixing ABL air with FT air, which contains considerable background concentrations of methane and carbon monoxide, leads to a higher hydrocarbon to NO_x ratio and therefore again to higher O_3 production efficiencies.

Therefore, the export of O_3 precursors from the ABL to the FT is a crucial component of the total tropospheric ozone budget. Exchange between the ABL and the FT occurs by processes ranging from synoptic systems, squall lines, deep and shallow cumulus and dry convection down to turbulence (Fiedler, 1982). Of these, only synoptic systems are resolved in GCTMs, with typical horizontal grid resolutions of $\sim 5^\circ \times 5^\circ$, whereas all other processes have to be parameterized. Vertical transport by deep, moist convection has been quantified in the last two decades (Cotton et al., 1995) and is parameterized in GCTMs (Jacob et al., 1997). Its influence on global O_3 budgets, however, is still under debate (Lelieveld and Crutzen, 1994). Parameterizations of dry, shallow convection in GCTMs assume ABL mixing, and hold for flat and homogeneous terrain. Above complex terrain (mountainous or coastal), however, thermal wind systems in the range of 0.1 to 100 km develop due to differential heating or cooling of the Earth's surface during clear sky and strong radiation conditions with weak synoptic forcing (fair weather). Export of trace gases from the ABL in complex terrain to the FT occurs through gaps in the ABL inversion (Kossmann et al., 1999), called topographic venting in the following. Once in the FT, pollutants might be re-circulated regionally on a time scale of a few days (Millan et al., 2002; Tyson and D'Abreton, 1998). Elevated layers in the FT are frequently observed (McKendry and Lundgren, 2000; Newell et al., 1999), indicating long-range transport of ABL constituents. Entrainment of elevated pollution layers into the ABL leads to increased surface pollutant concentrations at remote sites (Berkowitz et al., 2000).

This paper investigates the mechanism of topographic venting within deep Alpine valleys. Air mass export from the ABL to the FT is quantified by means of air mass budgets. Pollutant export and ozone chemistry will be discussed in a forthcoming paper.

2. Measurements and methods

2.1. Experimental setup

The VOTALP (Vertical ozone transport in the Alps) (Wotawa and Kromp-Kolb, 2000) and CHAPOP (Characterization of high Alpine pollution plumes) field campaigns took place in the Mesolcina and Leventina valleys in the southern Swiss Alps Fig. 1. The Leventina valley leads to the San Gottardo road tunnel and the Mesolcina valley to the San Bernardino road tunnel. Steep slopes (slope angle between 20° and 25°), small floor width (0.3 km to 1.0 km) and large depth (1.5 km to 2.0 km) are characteristic of both valleys. Major transalpine traffic routes within the Mesolcina and Leventina valley (~500 (Mesolcina) and ~4500 (Leventina) trucks per working day) represent a substantial NO_x source at the valley floor of approximately 1 and 10 kg (N) km^{-1} d^{-1}, respectively.

The measurement setup of the VOTALP Mesolcina study is described in detail by Furger et al. (2000). During the CHAPOP Leventina experiment multiple aircraft were used to investigate the structure and chemical composition of the valley's atmosphere. On three flight days (26 - 28 August 2001) a small research aircraft (Neininger et al., 2001) operated by the Swiss MetAir acquired meteorological, chemical and aerosol parameters by flying cross sections within the valley (thick black lines in Fig. 1). The MERLIN IV research aircraft (Meteo France) flew a box grid pattern at an altitude of 3–4 km a.s.l., measuring parameters similar to the MetAir aircraft. The FALCON research aircraft of the German Aerospace Center (DLR) carried a nadir-pointing aerosol lidar (Sect. 2.3) at a height of 8 km a.s.l. that supplied information about ABL struc-

ture, ABL development, and aerosol distribution. Radiosondes measuring atmospheric pressure, temperature, humidity, and wind (ZEEMET^{TM} Mark II MICROSONDE) were launched in the center of the valley. Continuous measurements of standard chemical and meteorological surface parameters were conducted during five weeks (August and September 2001) at three sites, including formaldehyde and detailed VOC analysis. Meteorological data was gathered at two additional sites at the valley's north-eastern slope. A sodar wind profiling system (Remtech, PA2) was situated at the north-eastern crest of the Leventina valley (Monte Matro, 2172 m a.s.l., eastern side of lidar transect c in Fig. 1) and acquired three-dimensional flow data up to 1 km above ground level.

2.2. Mass budget

We conducted air mass budget calculations for thermal airflow in the Mesolcina and Leventina valley to quantify vertical air mass export to the FT during daytime, fair weather conditions. Differential heating within a mountainous environment results in up-valley airflow parallel to the valley floor during the day (valley breeze). At the valley sidewalls, up-slope winds prevail (Whiteman, 2000), potentially penetrating the ABL inversion and resulting in export of polluted ABL air.

Vertical wind velocities in thermal updrafts or slope flows can be as high as a few meters per second. However, they are also often spatially and temporally intermittent. Estimating the vertical mass flux out of a valley atmosphere due to slope winds and vertical updrafts by direct measurements of the vertical wind velocity is therefore a difficult task. In this work we use an indirect method to determine the vertical mass export from the ABL within the valley breeze system to the FT as a residual of horizontal flow measurements.

For budget calculation purposes, a valley segment is composed of a minimum of three open interfaces, two vertical cross-sections within the main valley and a horizontal lid. Additional flow into or out of tributary valleys F_T has to be considered. Due to conservation of mass, the net vertical mass flux F_z is governed by the convergence of the horizontal mass fluxes $F_{y,out} - F_{y,in}$, F_T and the change of the valley breeze layer

air mass with time F_{VBL}

$$F_z = F_{y,out} - F_{y,in} + F_T - F_{VBL}. \quad (1)$$

Figure 2 shows an example of the air flow in the Leventina valley in two cross sections across the valley. Note that up-valley flow is indicated by negative sign and that no tributary valleys are present. Two contrary motions contribute to the net vertical mass flux. During daytime, strong upward motion occurs within the slope wind layer which is only partly balanced by sinking motion in the valley center. Mass balance closure is primarily obtained by the horizontal valley breeze flow.

The flow in the slope wind layer depends on the energy input to this layer by the sensible heat flux at the slope surface, atmospheric stability and the slope angle. The larger the sensible heat flux at the slope surface, the stronger the temperature differences between the valley center and the slope layer, providing the driving force for the slope winds. On the other hand, vertical motion is damped with increasing atmospheric stability. But near neutral stability prevents the generation of an organized slope wind due to enhanced turbulent vertical mixing (Vergeiner and Dreiseitl, 1987). Maximal upward flow was simulated in atmospheric numerical models for intermediate atmospheric stability (Atkinson and Shahub, 1994).

Mass budget calculations of the daytime valley breeze system have to date only been conducted for the broad Alpine Inn valley (Austria), which possesses important tributary valleys (Freytag, 1987). The valleys investigated in this study are narrow and have no tributaries, hence reducing the number of assumptions and making budget analyses more robust. Only the horizontal mass fluxes $F_{y,in}, F_{y,out}$ and the change of the valley breeze layer air mass with time F_{VBL} have to be measured to yield the vertical mass flux F_z . The horizontal mass flux through a valley segment is computed using wind data collected by the MetAir aircraft. A 5-hole gust probe (Keller capacitive sensors) provides three-dimensional wind data with a precision of 0.5 m s^{-1} for each component and a temporal resolution of 1 s. The wind velocity parallel to the valley axis v_p is horizontally averaged for layers of 50 m vertical extent, providing an individual vertical profile at each cross section (Fig. 3). The same procedure is done for the air density.

Integration from the valley floor h_0 up to the height h_t, where the valley breeze ceases and v_p changes sign (Fig. 3), yields the horizontal mass flux

$$F_y = \int_{h_0}^{h_t} \rho(z) \cdot v_p(z) \cdot B(z) dz, \quad (2)$$

where $B(z)$ is the valley width at height z. In the cases investigated in this study, the wind direction above the valley breeze layer was always opposite to the valley breeze flow. Hence, v_p always changed sign at the valley breeze top. Even if the flow above the valley breeze is in the same direction as the valley breeze itself, a minimum in the wind velocities between both layers and atmospheric stability changes with height can usually be observed and used to determine h_t. The mean uncertainty of an individual horizontal mass flux calculation due to the wind measurement uncertainty can be shown to be ± 7 %. Measurements at two cross sections are not done at the same time. A temporal correction for the horizontal mass flux is applied by using its temporal evolution derived from subsequent flights.

For nighttime drainage flows, different methods to quantify F_y have been used in other studies, showing uncertainties arising from individual vertical profile measurements (King, 1989). In contrast, individual vertical profiles used in this study do not represent a vertical profile above a single point at the cross section, but represent an average for the whole cross section. Horizontal mass fluxes were calculated with the individual vertical profile method and from two-dimensional interpolations of the measured wind data at the cross sections. Both methods varied only ± 7 to 11 % from each other, depending on interpolation scheme (Kriging, Inverse-Distance or Linear interpolation) and parameter settings (scaling of vertical to horizontal distance).

The change of the valley breeze layer air mass with time is governed by the change of the valley breeze layer height with time (Fig. 3)

$$F_{VBL} = \frac{m_V\left(h_l\left(t_2\right)\right) - m_V\left(h_l\left(t_1\right)\right)}{t_2 - t_1}, \quad (3)$$

where h_l is the mean height of valley breeze layer at the lower and the upper cross section. The valley's air mass, m_V, is derived from digitized topographic data and for standard atmospheric conditions. The time difference, $t_2 - t_1$, between two cross-sectional flights was typically about two hours. During the VOTALP campaign valley-parallel wind velocities were continuously measured with scintillometers (Poggio et al., 2000), showing only small variations in the average up-valley flow during daytime. In addition, the wind velocity measured within 10-minute intervals at surface stations in the Leventina valley deviated only by 16 % from the two-hour averages. This underlines the stationary upvalley flow and justifies the assumptions made for the mass budget calculation. In contrast, an observational and numerical study in the nearby Riviera valley shows that the structure and intensity of the valley breeze undergoes significant changes during the day and shows intermittent character (De Wekker et al., 2003). This might be due to different valley configuration and different synoptical forcing. For mass budget calculations like the one presented here the spatial and temporal homogeneity of the valley breeze has to be inspected.

2.3. Lidar

The nadir-pointing backscatter lidar, operated by the DLR (Kiemle et al., 1995), was used to observe the structure of the ABL at the wavelength λ = 354, 532 and 1064 nm. The backscatter ratio β, which is determined by the lidar, is the ratio of the total backscatter (Mie + Rayleigh) to Rayleigh backscatter. Since high relative humidity (RH) values lead to aerosol growth and therefore enhanced Mie scatter, β is enhanced in regions with high aerosol concentration and high RH. Hence, a direct comparison in terms of aerosol concentrations between different altitudes and distant regions is not possible.

2.4. Forward trajectories

To analyze the pathways of pollutants exported to the FT, forward trajectories were initialized at three sites north and south of the main Alpine crest and at different altitudes. We used the FLEXTRA trajectory model (Stohl et al., 1995) based on European Center for Medium-Range Weather Forecasts (ECMWF) analysis.

For the years 2000 and 2001, days that were favorable for topographic venting were selected. Since the energy flux at the Earth's surface plays a very important role in supporting thermal wind systems a simple criterion to select fair weather days was chosen. Days with more than 9 hours of sunshine at selected stations at the northern and the southern side of the main Alpine crest within Switzerland were selected. Ten stations, covering the whole Swiss plateau, and four stations, covering the Ticino area in the south, were chosen. 50 % of the northern stations and 50 % of the southern stations had to fulfill the criterion. A total of 101 days within the two-year period were selected. The selected days lie in the period from the end of March to the beginning of October. Sunshine data was taken from the automatic network of meteorological observations maintained by the Swiss national weather service (MeteoSwiss).

3. Results

3.1. Export of boundary layer air

Horizontal mass fluxes and the change of the valley breeze layer mass with time were computed from a database of 8 flights within both valleys and from digitized topographic information. In order to compare the vertical mass fluxes estimated with the budget method these fluxes are normalized by the length of the investigated valley segment and the air mass of the valley breeze layer, respectively. In this way, the mass export per unit valley length and the fraction of ABL air exported per hour is obtained for each valley. We derived an average net vertical export of 33 % of the valley breeze

layer air mass per hour (Table 1). This export rate is similar in both Mesolcina and Leventina valleys, and was somewhat higher in June compared to July and August. In June the vertical mass flux per valley length $F_{z,N}$ is twice as high as in July and August. On the other hand the valley breeze layer height was also larger in June so that the export rate is only one third larger in June compared to July and August. These differences are probably due to weaker atmospheric stability in June.

Valley breeze conditions persist for about 7 - 9 h d^{-1} during the summer season at this latitude, resulting in venting to the lower FT of 2.3 - 3.0 times the valley breeze layer air mass per day.

3.2. Boundary layer structure

Figures 4 to 6 shows a sequence of three cross-valley transects from north (Fig. 4) to south (Fig. 6) within the Leventina valley. Two different aerosol layers are evident. The area below 1100 m a.s.l. can be interpreted as the convective boundary layer within the valley. Comparison with balloon soundings of potential temperature θ and specific humidity q (Fig. 4) shows that the height of the convective boundary layer is even below the altitude of high β. The convective boundary layer is visually indicated by constant to decreasing θ with height and large specific humidity. The convective boundary layer height shown here is relatively low compared to other days. Unfortunately there are no backscatter data available on other days. Typically, a height of 2000 m a.s.l. was observed from potential temperature profiles. Above 1600 m a.s.l. within the second layer, which reaches up to 4.1 km a.s.l., the prevailing wind was coming from west to northwest. This can be seen in Fig. 7, showing wind data measured by the MERLIN IV at an altitude of ~3900 m a.s.l. Horizontally averaged backscatter ratios increased from northwest to southeast (Fig. 7), indicating the additional injection of ABL air into the second layer while being advected horizontally by the synoptic flow. Increased backscatter ratios are also observed in the slope wind layer (Figs. 5, 8), indicating up-slope transport of aerosols and moisture from the ABL.

Assuming that the whole vertical mass flux, as derived by the budget method, occurs within the slope wind system, the corresponding slope wind depth was evaluated. Typical slope wind velocities measured during the CHAPOP campaign were ∼2 m s^{-1}. The estimated slope wind depth of ∼100 m is similar to depths observed directly in other studies (Kossmann et al., 1999). This suggests that slope winds are the most important mechanism for vertical export of ABL air. This is also supported by strong upward motion observed by the sodar wind profiling system (Fig. 9) above the crest, where the winds of both slopes merge. Vertical velocities of more than ∼1.5 m s^{-1} can be seen from 10:00 UTC to 16:00 UTC ranging up to 700 m above ground level. During the night sinking motion persists due to the larger scale subsidence and possibly local down-slope flow. However, the downward motion during the night is much weaker than the upward motion during the day.

Ground based lidar observations in the Mesolcina valley during VOTALP showed an increase in backscatter ratios above crest height in the afternoon hours (Carnuth and Trickl, 2000). In addition, the increase of VOC concentrations above crest height between morning and afternoon could be related to vertical transport of in-valley traffic emissions (Prevot et al., 2000). In other studies, elevated layers have been observed downwind of the Alps and over the Adriatic Sea (Nyeki et al., 2002), indicating horizontal transport of ABL air masses that might have been lifted above mountainous terrain. Even further away above the Mediterranean elevated layers are frequently observed (Lelieveld et al., 2002), caused by other lifting processes including topographic venting.

3.3. Forward trajectories

On days with fair weather conditions for the years 2000 and 2001, two ensembles of forward trajectories with an initial altitude of 3500 m a.s.l. were identified (Figs. 10 and 11). This altitude corresponds with the altitude that is reached by topographic venting. In the first ensemble, air masses move in a southerly direction and slowly descend within the subtropical anticyclone above the Mediterranean and North Africa.

Contained pollutants possibly influence surface concentrations or remain in reservoir layers (Lelieveld et al., 2002; Traub et al., 2003). In the second ensemble, air masses move northward and ascend up to 9000 m a.s.l. influencing the whole tropospheric column, experiencing increased westerly flow and leading to transport towards Asia. These results look similar for all three sites where trajectories were initialized. However, the results change for different initial altitudes (Fig. 12). North of the Alps the differences in initial altitudes disappear. South of the Alps lower initial altitudes cause the air to descend faster and travel slower southwards than for higher initial altitudes. Only 1 % of all forward trajectories initialized below 2 km a.s.l. reach the FT south of 20° N within 8 days. In contrast, 10 % of trajectories initialized at 3500 m a.s.l. arrive in the same region and within the same time, and begin to ascend in the intertropical convergence zone (ITCZ) potentially reaching the upper troposphere and lower stratosphere. Obviously, this pathway for European ABL pollutants is a result of preceding topographic venting above the Alps.

4. Discussion

Our investigations of the daytime valley atmosphere under fair weather conditions are schematically summarized in Fig. 13. Pollutants are emitted mainly at the valley floor or advected horizontally by the valley breeze from the forelands. Within the valley, a well-mixed boundary layer (NO_x mixing ratios of about 10 ppbv) is capped by a rather stable layer indicated by an increase of potential temperature (dashed-dotted line). Up-slope winds are able to penetrate this layer and lift polluted air from lower levels. Additional shallow cumulus cloud formation above the crests further maintains vertical motion. Above the stable layer horizontal airflow is mainly synoptically driven. In contrast to the ABL, the upper layer is only partly mixed and is indirectly connected to the surface, therefore the term “injection layer” is used (NO_x ~1 ppbv). The injection layer is capped by a strong inversion that marks the transition to the FT (NO_x ~0.1 ppbv). The mass balance of the slope flow system is not closed in the two-dimensional valley cross sec-

tion but in a three dimensional way by the valley breeze.

Extrapolating the high export rates derived for the Leventina and the Mesolcina valleys to the whole Alpine region, we estimated the total NO_x export by thermal wind systems in the Alps. A calculation that considers advection from the forelands, accumulation of nighttime emissions in the ABL, but no day-to-day accumulation or chemical transformation, yields an estimated total NO_x export of ~0.2 Gg(N) per day. This corresponds to ~50 % of daily NO_x emissions in the region influenced by plain-to-mountain flows (area enclosed by the thin white line in Fig. 1). The annual average NO_x + PAN export of the European ABL has been estimated at 21 % of total emissions using a GCTM (Wild and Akimoto, 2001). This suggests that on fair weather days pollutant export by thermal wind systems enhances export by a factor of ~2.5 in the Alps. This enhancement, yet unconsidered in GCTMs, will also occur within other European mountainous regions, such as the Pyrenees and Apennines.

O_3 concentrations in the ABL are typically high (> 80 ppbv O_3) for the investigated weather conditions and for air masses advected from the Po Basin (Prevot et al., 1997). Heavy goods and passenger traffic through the Swiss Alps have increased by 72 % and 18 % in the last decade, respectively, and are expected to grow in the future. Due to enhanced O_3 production efficiency in the FT (~25 (molec. O_3) / (molec. NO_x) in the spring time FT above the Alps (Carpenter et al., 2000) and ~5 (molec. O_3) / (molec. NO_x) in the European ABL (Hov and Flatoy, 1997)) and rapid vertical transport, a NO_x molecule emitted in an Alpine valley and lifted to the FT produces more O_3 than a NO_x molecule above flat terrain. Therefore considerable amounts of O_3 are exported directly and indirectly to the FT.

5. Conclusions

Topographic venting of ABL air from deep Alpine valleys to the FT was quantified from observed air mass budgets for two Alpine valleys during three aircraft campaigns. As

much as 3 times the valley breeze layer air mass is exported on a summer time fair weather day. Observations of atmospheric backscatter ratios observed by an airborne lidar confirm this venting mechanism. Pollutants and moisture are exported from the ABL within the valley to the injection layer. This layer reaches up well above crest height to about 4000 m a.s.l. Our observations also suggest that daytime slope winds are the main mechanism driving vertical export. Pollutants trapped in the injection layer leave the mountainous terrain well above the ABL of the forelands, and therefore become part of the FT. About 50 days with strong solar insolation within the summer months favor topographic venting. Trajectory studies for these days show that the initial height above the Alps determines how fast and at which altitude an air mass is transported southward, exporting European air pollutants which were lifted by topographic venting above the Alps.

Topographic venting is expected to play a more important role in Europe than in North America and Asia where pollutant export is influenced more strongly by warm conveyer belts (upward airflow within extratropical cyclone ahead of the cold front) that are less frequently observed in Europe (Stohl, 2001).

Since 27 % of the Earth's land surface is defined as mountainous (altitude > 1500 m a.s.l.) (Messerli and Ives, 1997) and mountain ranges lower than the Alps tend to force thermal convection as well (Kossmann et al., 1999), topographic venting is not only of regional European but of global importance. However, complex topography is only treated on a sub-grid scale in GCTMs, consequently topographic venting is not represented properly (Noppel and Fiedler, 2002). Development of a suitable topographic venting parameterization for GCTMs will help to better quantify the effects of thermal air flow in mountainous terrain on continental and global tropospheric pollution budgets.

Investigations on a climatological scale, e.g. long term lidar studies or analysis of operationally available sounding data, could verify the significance of the topographic venting mechanism. The chemical composition of the ABL and the injection layer was analyzed during both VOTALP and CHAPOP campaign. The gathered information will be used to quantify the expected O_3 production efficiency enhancement in an air mass

lifted to the injection layer.

Acknowledgements. Support by the European Commission for the projects VOTALP and CAATER is acknowledged. Ground based meteorological data and flight planing support was provided by MeteoSwiss. Special thanks go to V. Fumagalli and the Kanton Ticino for supporting the build-up of the measurement sites during the CHAPOP campaign. We also like to thank the crews or the DLR Falcon, the Meteo France MERLIN IV, the MetAir and all involved groups in both projects.

References

Atkinson, B. W. and Shahub, A. N.: Orographic and Stability Effects on Daytime, Valley-Side Slope Flows, Boundary-Layer Meteorology, 68, 275–300, 1994. 5210

Berkowitz, C. M., Fast, J. D., and Easter, R. C.: Boundary layer vertical exchange processes and the mass budget of ozone: Observations and model results, Journal of Geophysical Research-Atmospheres, 105, 14 789–14 805, 2000. 5207

Carnuth, W. and Trickl, T.: Transport studies with the IFU three-wavelength aerosol lidar during the VOTALP Mesolcina experiment, Atmospheric Environment, 34, 1425–1434, 2000. 5215

Carpenter, L. J., Green, T. J., Mills, G. P., Bauguitte, S., Penkett, S. A., Zanis, P., Schuepbach, E., Schmidtbauer, N., Monks, P. S., and Zellweger, C.: Oxidized nitrogen and ozone production efficiencies in the springtime free troposphere over the Alps, Journal of Geophysical Research, 105, 14 547–14 559, 2000. 5217

Cotton, W., Alexander, G., Hertenstein, R., Walko, R., McAnelly, R., and Nicholls, M.: Cloud venting – A review and some new global annual estimates, Earth-Science Reviews, 39, 169–206, 1995. 5207

De Wekker, S. F. J., Steyn, D. G., Fast, J. D., Rotach, M. W., and Zhong, S.: The Performance of RAMS in Representing the Convective Boundary Layer Structure in a Very Steep Valley, Environmental Fluid Mechanics, submitted, 2003. 5212

Fiedler, F.: Atmospheric Circulation, in Chemistry of the Unpolluted and Polluted Troposphere, edited by Georgii, H. W.and Jaeschke, W., 509, Reidel Publishing Company, Dordrecht, 1982. 5207

Freytag, C.: Results from the MERKUR Experimant: Mass Budget and Vertical Motions in a

Large Valley During Mountain and Valley Wind, Meteorology and Atmospheric Physics, 37, 129–140, 1987. 5210

Furger, M., Dommen, J., Graber, W., Poggio, L., Prévôt, A., Emeis, S., Grell, G., Trickl, T., Gomiscek, B., Neininger, B., and Wotawa, G.: The VOTALP Mesolcina Valley Campaign 1996 – concept, background and some highlights, Atmospheric Environment, 34, 1395–1412, 2000. 5208

Hov, O. and Flatoy, F.: Convective redistribution of ozone and oxides of nitrogen in the troposphere over Europe in summer and fall, Journal of Atmospheric Chemistry, 28, 319–337, 1997. 5217

Jacob, D. J., Prather, M. J., Rasch, P. J., Shia, R. L., Balkanski, Y. J., Beagley, S. R., Bergmann, D. J., Blackshear, W. T., Brown, M., Chiba, M., Chipperfield, M. P., deGrandpre, J., Dignon, J. E., Feichter, J., Genthon, C., Grose, W. L., Kasibhatla, P. S., Kohler, I., Kritz, M. A., Law, K., Penner, J. E., Ramonet, M., Reeves, C. E., Rotman, D. A., Stockwell, D. Z., VanVelthoven, P. F. J., Verver, G., Wild, O., Yang, H., and Zimmermann, P.: Evaluation and intercomparison of global atmospheric transport models using Rn-222 and other short-lived tracers, Journal of Geophysical Research-Atmospheres, 102, 5953–5970, 1997. 5207

Kiemle, C., Kastner, M., and Ehret, G.: The Convective Boundary-Layer Structure from Lidar and Radiosonde Measurements During the Efeda-91 Campaign, Journal of Atmospheric and Oceanic Technology, 12, 771–782, 1995. 5212

King, C. W.: Representativeness of Single Vertical Wind Profiles for Determining Volume Flux in Valleys, Journal of Applied Meteorology, 28, 463–466, 1989. 5211

Kossmann, M., Corsmeier, U., De Wekker, S., Fiedler, F., Vögtlin, R., Kalthoff, N., Güsten, H., and Neininger, B.: Observations of Handover Processes between the Atmospheric Boundary Layer and the Free Troposphere over Mountainous Terrain, Contributions to Atmospheric Physics, 72, 329–350, 1999. 5207, 5215, 5218

Lelieveld, J. and Crutzen, P. J.: Role of Deep Cloud Convection in the Ozone Budget of the Troposphere, Science, 264, 1759–1761, 1994. 5207

Lelieveld, J., Berresheim, H., Borrmann, S., Crutzen, P. J., Dentener, F. J., Fischer, H., Feichter, J., Flatau, P. J., Heland, J., Holzinger, R., Korrmann, R., Lawrence, M. G., Levin, Z., Markowicz, K. M., Mihalopoulos, N., Minikin, A., Ramanathan, V., de Reus, M., Roelofs, G. J., Scheeren, H. A., Sciare, J., Schlager, H., Schultz, M., Siegmund, P., Steil, B., Stephanou, E. G., Stier, P., Traub, M., Warneke, C., Williams, J., and Ziereis, H.: Global air pollution crossroads over the Mediterranean, Science, 298, 794–799, 2002. 5215, 5216

Lin, X., Trainer, M., and Liu, S. C.: On the Nonlinearity of the Tropospheric Ozone Production, Journal of Geophysical Research, 93, 15 879–15 888, 1988. 5206
McKendry, I. G. and Lundgren, J.: Tropospheric layering of ozone in regions of urbanized complex and/or coastal terrain: a review, Progress in Physical Geography, 24, 329–354, 2000. 5207
Messerli, B. and Ives, J. (Eds.): Mountains of the World: A Global Priority, Parthenon, New York & London, 1997. 5218
Millan, M. M., Sanz, M. J., Salvador, R., and Mantilla, E.: Atmospheric dynamics and ozone cycles related to nitrogen deposition in the western Mediterranean, Environmental Pollution, 118, 167–186, 2002. 5207
Neininger, B., Fuchs, W., Baeumle, M., Volz-Thomas, A., Prévôt, A., and Dommen, J.: A small aircraft for more than just ozone: METAIR's 'DIMONA' after ten years of evolving development, in 11th Symposium on Meteorological Observations and Instrumentation, American Meteorological Society, Albuquerque, NM, USA, 2001. 5208
Newell, R. E., Thouret, V., Cho, J. Y. N., Stoller, P., Marenco, A., and Smit, H. G.: Ubiquity of quasi-horizontal layers in the troposphere, Nature, 398, 316–319, 1999. 5207
Noppel, H. and Fiedler, F.: Mesoscale heat transport over complex terrain by slope winds – A conceptual model and numerical simulations, Boundary-Layer Meteorology, 104, 73–97, 2002. 5218
Nyeki, S., Eleftheriadis, K., Baltensperger, U., Colbeck, I., Fiebig, M., Fix, A., Kiemle, C., Lazaridis, M., and Petzold, A.: Airborne lidar and in-situ aerosol observations of an elevated layer, leeward of the European Alps and Apennines, Geophysical Research Letters, 29, 1852, 2002. 5215
Poggio, L. P., Furger, M., Prevot, A. S. H., Graber, W. K., and Andreas, E. L.,: Scintillometer wind measurements over complex terrain, Journal of Atmospheric and Oceanic Technology, 17, 17–26, 2000. 5212
Prevot, A. S. H., Staehelin, J., Kok, G. L., Schillawski, R. D., Neininger, B., Staffelbach, T., Neftel, A., Wernli, H., and Dommen, J.: The Milan photooxidant plume, Journal of Geophysical Research-Atmospheres, 102, 23 375–23 388, 1997. 5217
Prevot, A. S. H., Dommen, J., and Baeumle, M.: Influence of road traffic on volatile organic compound concentrations in and above a deep Alpine valley, Atmospheric Environment, 34, 4719–4726, 2000. 5215
Seinfeld, J. H. and Pandis, S. N.: Atmospheric chemistry and physics, Wiley, New York, 1998.

5206
Stohl, A.: A 1-year Lagrangian "climatology" of airstreams in the Northern Hemisphere troposphere and lowermost stratosphere, Journal of Geophysical Research-Atmospheres, 106, 7263–7279, 2001. 5218
Stohl, A., Wotawa, G., Seibert, P., and Kromp-Kolb, H.: Interpolation Errors in Wind Fields as a Function of Spatial and Temporal Resolution and Their Impact on Different Types of Kinematic Trajectories, Journal of Applied Meteorology, 34, 2149–2165, 1995. 5213
Traub, M., Fischer, H., de Reus, M., Korrmann, R., Heland, J., Ziereis, H., Schlager, H., Holzinger, R., Warneke, C., de Gouw, J. A., and Lelieveld, J.: Chemical characteristics assigned to trajectory clusters during the MINOS campaign, Atmospheric Chemistry and Physics Discussions, 3, 107–134, 2003. 5216
Tyson, P. D. and D'Abreton, P. C.: Transport and recirculation of aerosols off southern Africa - Macroscale plume structure, Atmospheric Environment, 32, 1511–1524, 1998. 5207
Vergeiner, I. and Dreiseitl, E.: Valley Winds and Slope Winds – Observations and Elementary Thoughts, Meteorology and Atmospheric Physics, 36, 264–286, 1987. 5210
Whiteman, C. D.: Mountain Meteorology, Oxford University Press, New York, 2000. 5209
Wild, O. and Akimoto, H.: Intercontinental transport of ozone and its precursors in a three-dimensional global CTM, Journal of Geophysical Research-Atmospheres, 106, 27 729–27 744, 2001. 5217
Wotawa, G. and Kromp-Kolb, H.: The research project VOTALP – general objectives and main results, Atmospheric Environment, 34, 1319–1322, 2000. 5208

Table 1. Net vertical mass export of the investigated valleys. Mean standard deviation of individual flux measurements is given in parentheses and derived from standard deviation of the up-valley wind velocity at each altitude level used for the horizontal flux calculation

Valley	Number of flights	$-F_{y,in}$ $(\frac{Tg}{h})$	$-F_{y,out}$ $(\frac{Tg}{h})$	F_{VBL} $(\frac{Tg}{h})$	F_z $(\frac{Tg}{h})$	$F^a_{z,N}$ $(\frac{Tg}{h\,km})$	Export rate[b] $(\frac{\%}{h})$
Leventina (August '01)	4	51 (3)	22 (3)	5.6	24 (4)	1.5 (0.3)	30 (5)
Mesolcina (July '96)	2	69 (5)	35 (1)	-1.4	35 (5)	1.8 (0.3)	28 (4)
Mesolcina (June '98)	2	113 (5)	38 (3)	3.2	71 (5)	3.7 (0.4)	42 (3)
Average	-	-	-	-	39	2.1	33

[a] The net vertical mass flux divided by the length of the valley segment.
[b] Percentage export of the valley breeze layer mass.

ACPD
3, 5205–5236, 2003

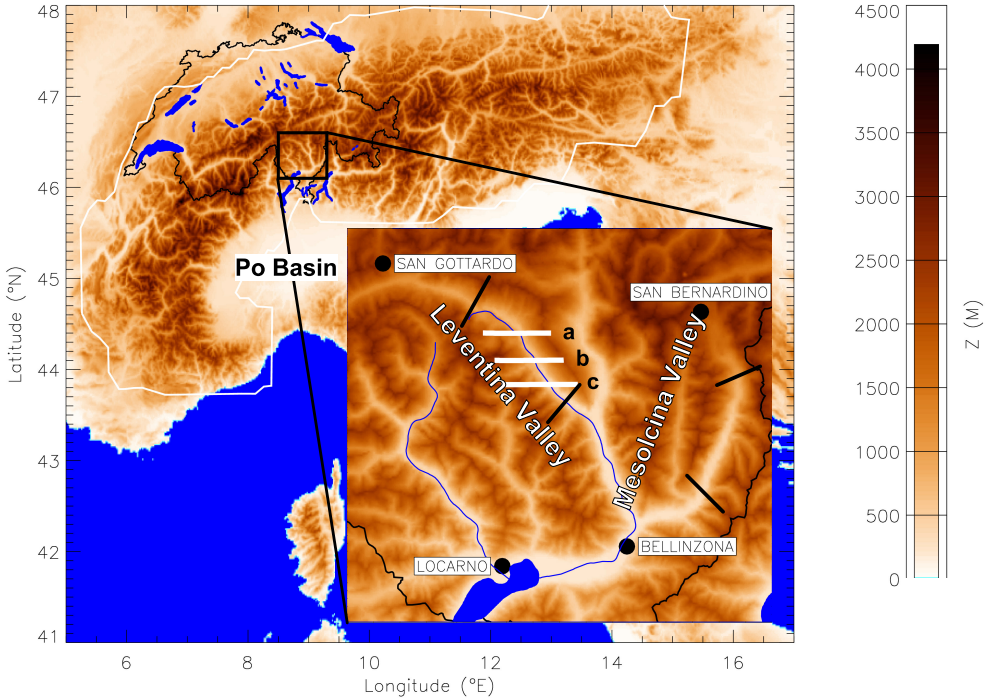

Fig. 1. Investigated valleys in southern Switzerland. White solid lines a–c indicate lidar transects above the Leventina Valley. Black solid lines represent cross-sectional flights of the MetAir aircraft used for the mass budget calculation.

ACPD
3, 5205–5236, 2003

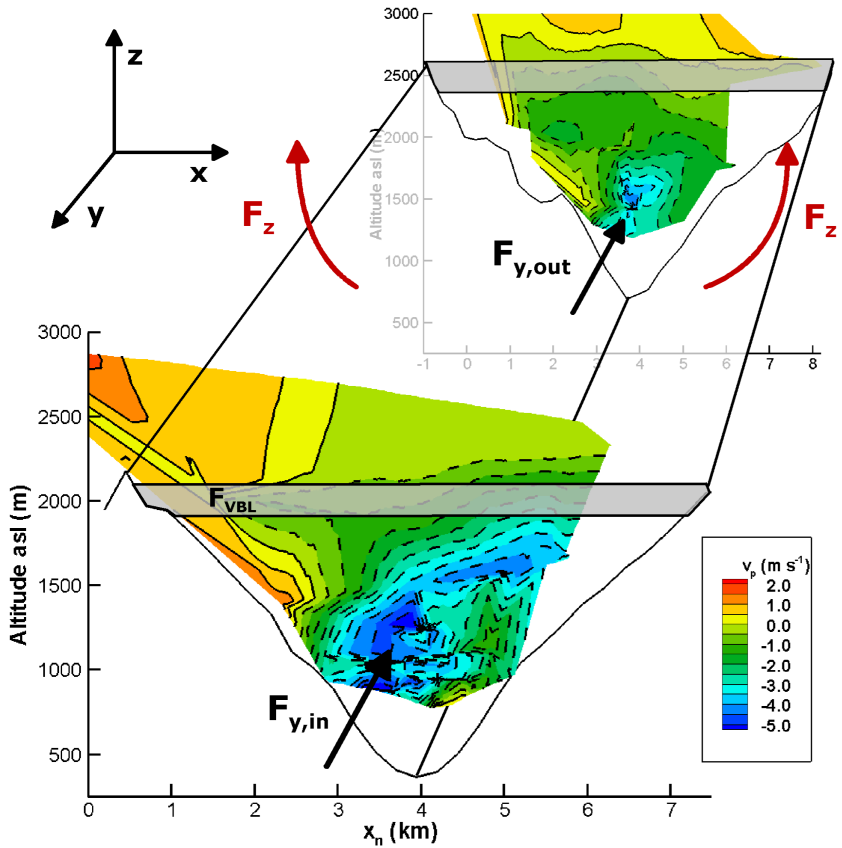

Fig. 2. Air flow in the Leventina valley at 10:00 UTC on 26 August 2001. Horizontal mass fluxes $F_{y,in}$ and $F_{y,out}$ and change of valley breeze layer air mass with time F_{VBL} as measured by the MetAir aircraft. The horizontal direction x_n is perpendicular to the valley axis, the y direction points down-valley. The contour plot depicts wind velocity parallel to the valley axis v_p. Negative values indicate up-valley flow, positive values down-valley flow.

ACPD
3, 5205–5236, 2003

Title Page
Abstract | Introduction
Conclusions | References
Tables | Figures
◀| |▶
◀ ▶
Back | Close
Full Screen / Esc
Print Version
Interactive Discussion

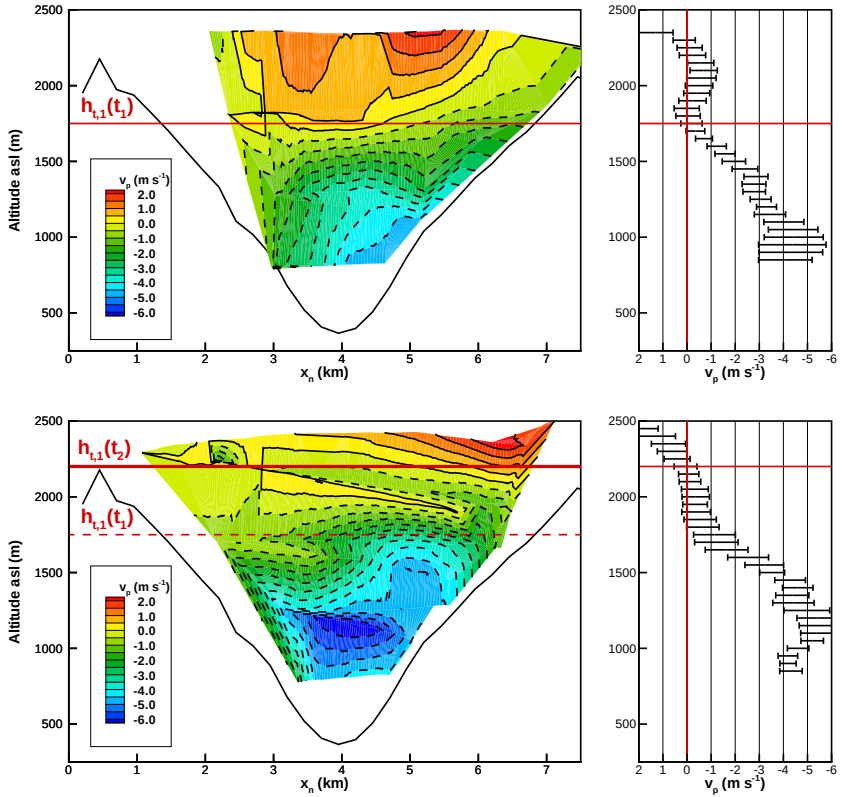

Fig. 3. Change of valley breeze with time. Contour plot (left) of valley parallel wind velocity v_p at cross-section within Leventina valley on 28 August 11:45 UTC (upper figures) and 13:30 UTC (lower figures) and vertical profile of horizontal averaged v_p (right). Change of valley breeze layer height z_{VBL} with time is indicated in lower figure. The example shows a rather strong change of the valley breeze layer height to illustrate the effect. Usually the change of the valley breeze layer height was much smaller.

ACPD
3, 5205–5236, 2003

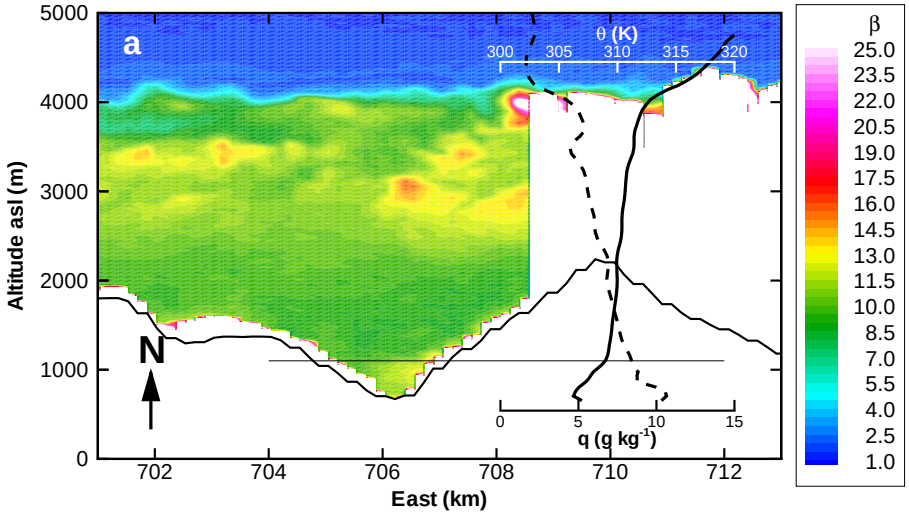

Fig. 4. Atmospheric backscatter ratio β for lidar transect within the Leventina valley on 28 August 2001 from 13:36 and 13:56 UTC, λ = 1064 nm. Horizontal coordinates refer to Swiss coordinate system. Transect corresponds to white solid lines labeled a in Fig. 1 and Fig. 7. The surface as seen by the lidar differs slightly from digitized topographic data with 250 m × 250 m horizontal resolution (black solid line). The lidar beam does not penetrate clouds, represented by white areas. Potential temperature θ (solid black line) and specific humidity q (dashed black line) as measured by a radio sonde launched at 12:00 UTC at the valley floor close to the transect are included.

ACPD
3, 5205–5236, 2003

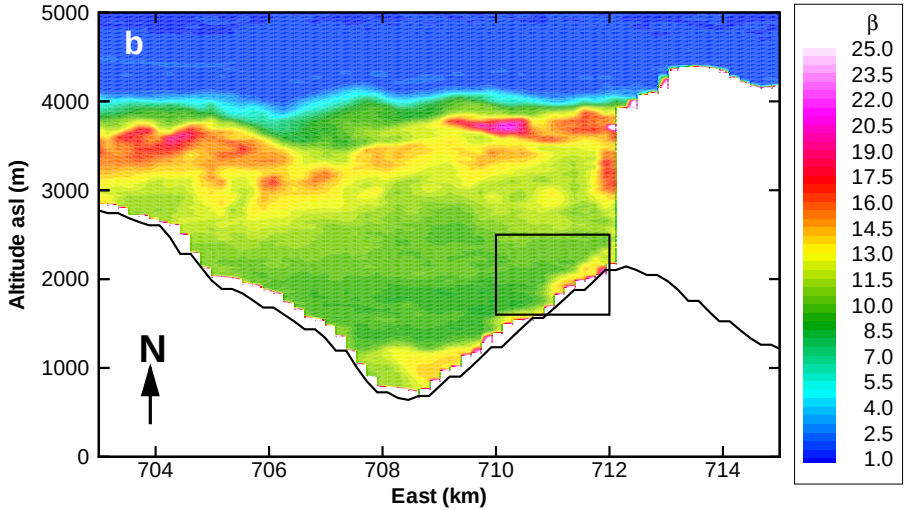

Fig. 5. Same as Fig. 4 but for transect b. See Fig. 8 for blow up of slope wind layer (black rectangle).

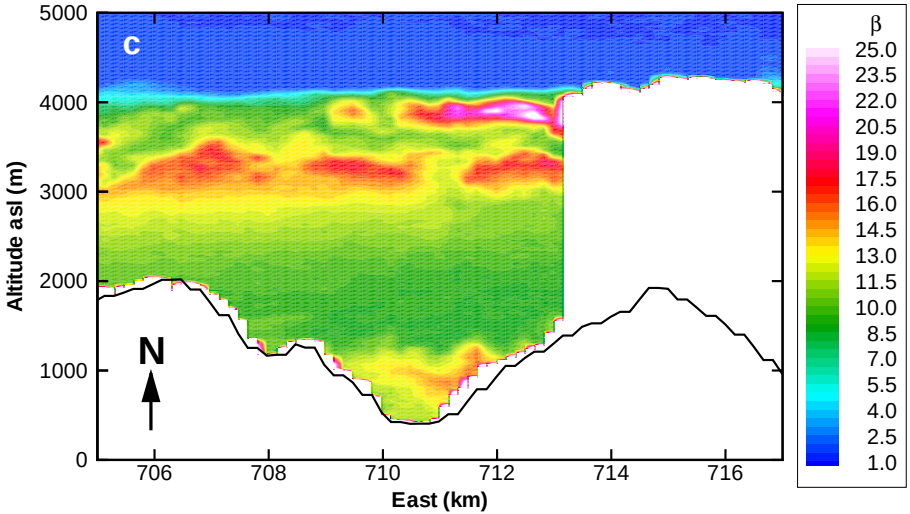

Fig. 6. Same as Fig. 4 but for transect c.

ACPD
3, 5205–5236, 2003

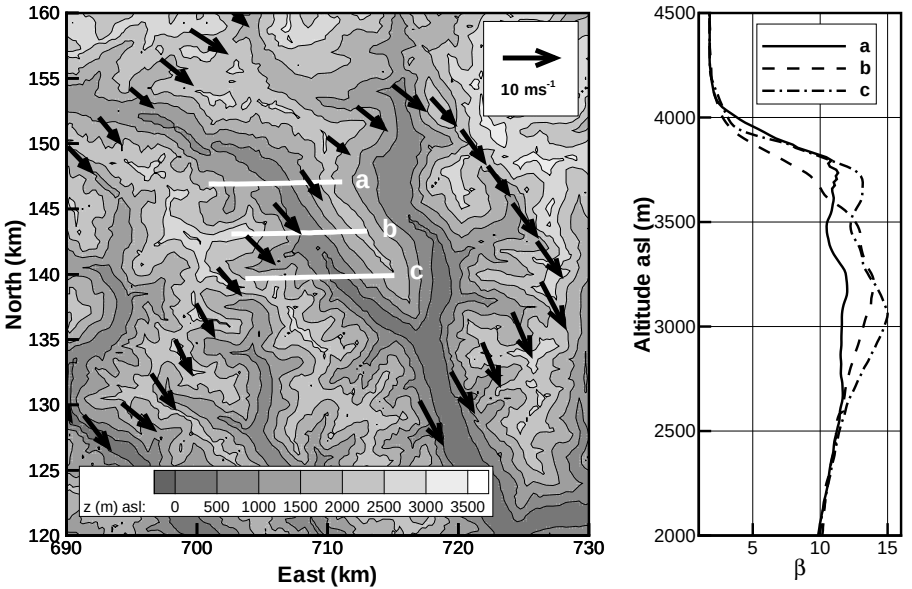

Fig. 7. Left: Flow at 3900 m a.s.l. above Leventina valley, 28 August 2001, 12:00 UTC. Coordinates refer to Swiss coordinate system. White solid lines represent lidar transects in Figs. 4 to 6. The length of the vectors are proportional to the wind velocity. Right: Mean vertical profiles of backscatter ratio β for transects a–c.

ACPD
3, 5205–5236, 2003

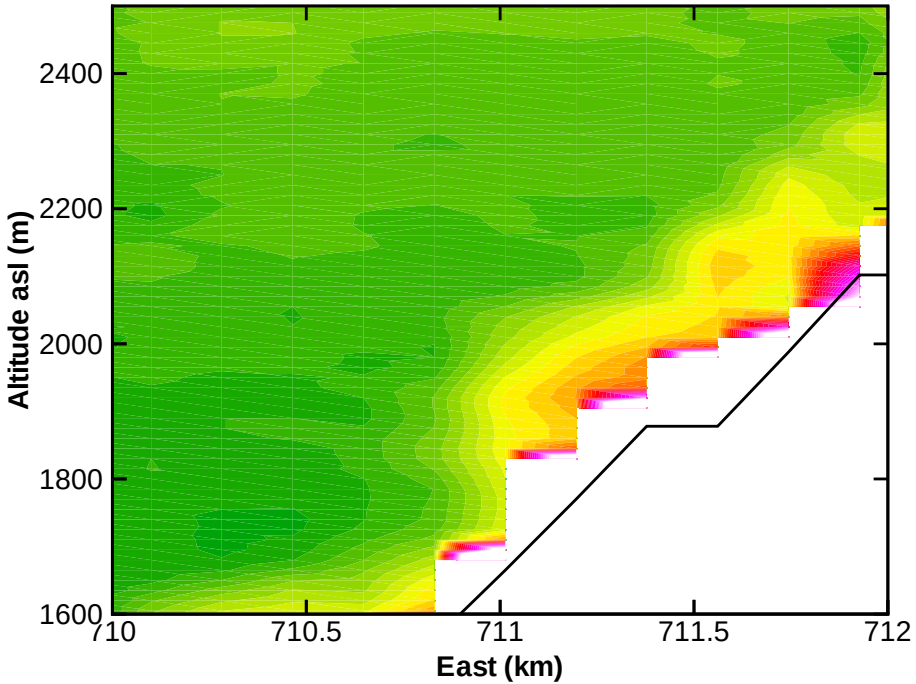

Fig. 8. Same as Fig. 5, but magnified slope wind layer.

ACPD
3, 5205–5236, 2003

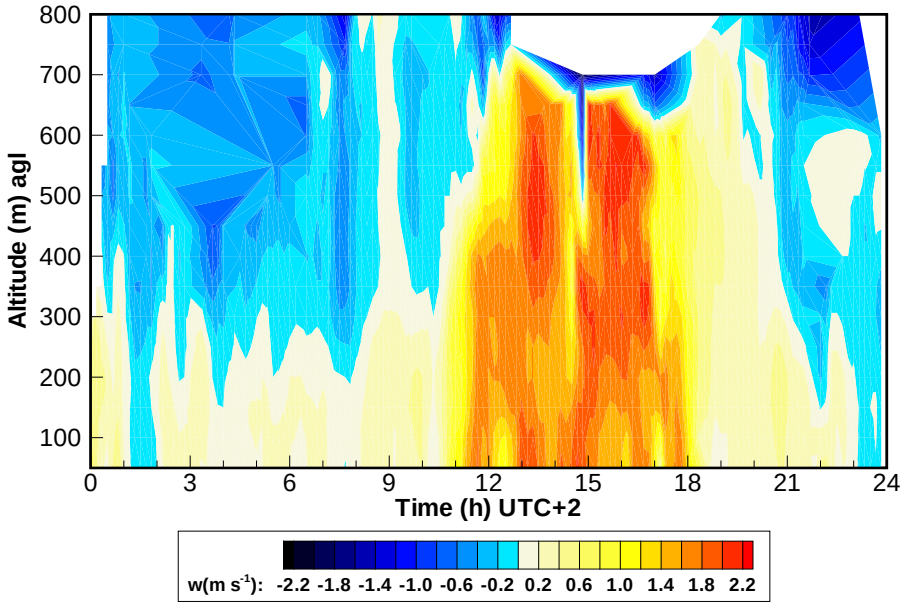

Fig. 9. Evolution of vertical wind velocities above the north-eastern crest of the Leventina valley on 28 August 2001. Yellow to red colors indicate upward motion, blue to black colors indicate downward motion.

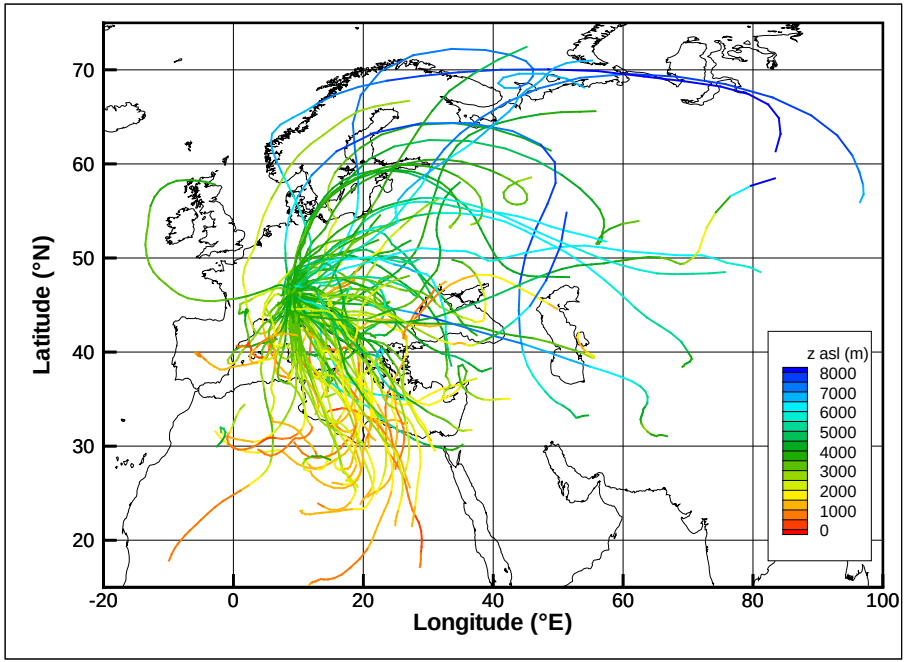

Fig. 10. Forward trajectories initialized at 3428 m a.s.l. above Gotthard region (8° 58' E, 46° 21' N) at 16:00 UTC on fair weather days for the years 2000 and 2001. Colors indicate the altitude of the air mass above sea level.

ACPD
3, 5205–5236, 2003

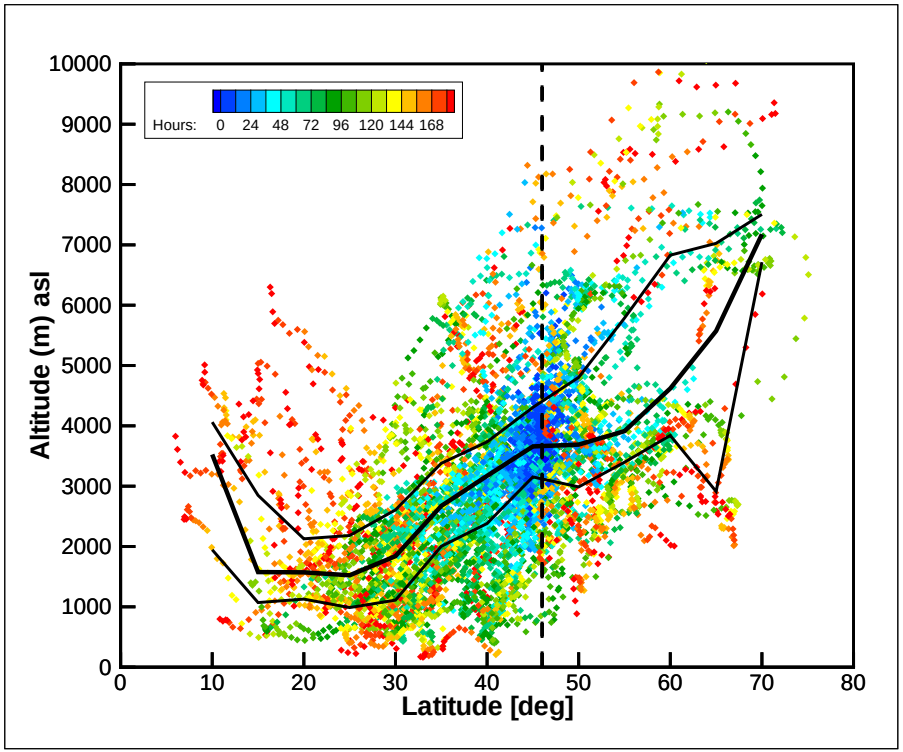

Fig. 11. Altitude of the trajectories shown in Fig. 10 versus latitude. Symbols represent individual trajectory points. Color coding refers to the hours since the trajectory was started. The black line indicates the median height of all trajectory points in 5° latitudinal bins. Thin black lines represent the corresponding lower and upper quartiles.

ACPD
3, 5205–5236, 2003

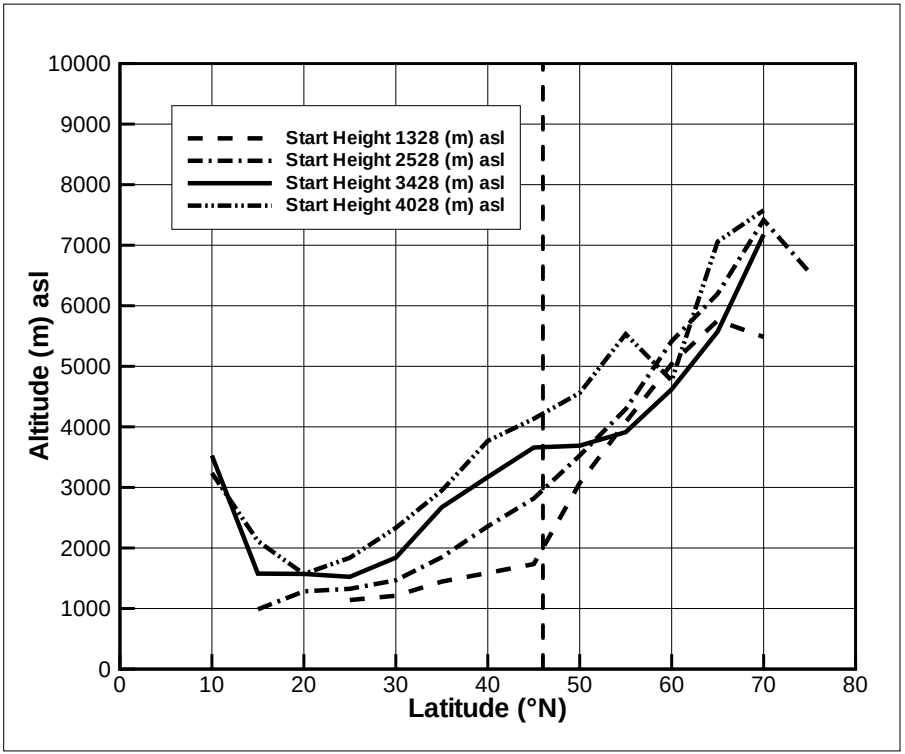

Fig. 12. Median altitude of trajectories versus latitude (5° bins). Ensembles with different initial altitudes.

ACPD
3, 5205–5236, 2003

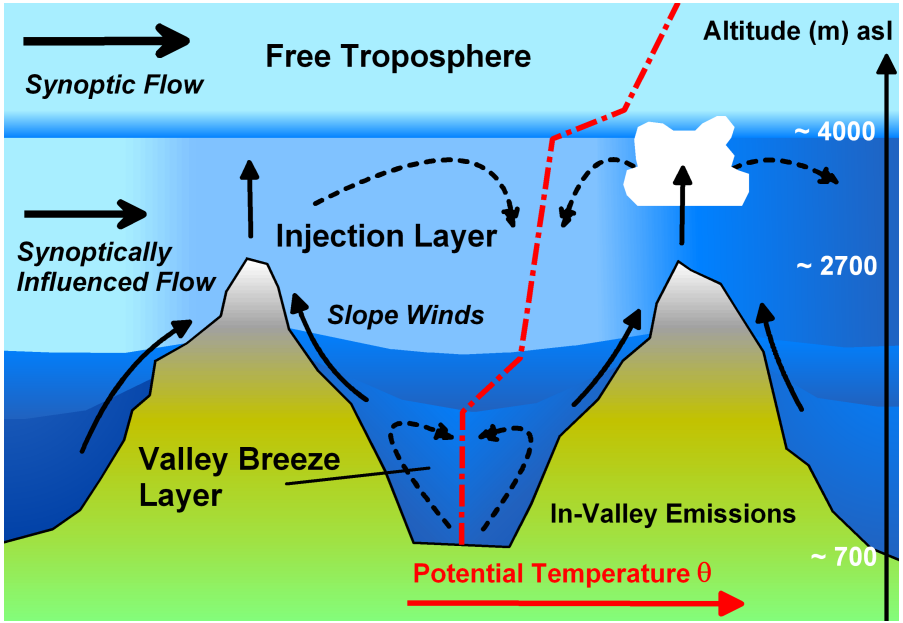

Fig. 13. Schematic of the daytime atmospheric structure and vertical pollution transport in and above deep Alpine valleys. Altitudes given represent typical values for the cases studied. Typical potential temperature profile is indicated by dashed red line. See text for details.

ACPD
3, 5205–5236, 2003